Higher Order Geometrical Modeling and Higher Order Field/Current Modeling in FEM, MoM, and PO Simulations

Branislav M. Notaroš, Milan M. Ilić, and Miroslav Djordjević
University of Massachusetts Dartmouth, Electrical and Computer Engineering Dept.
285 Old Westport Road, North Dartmouth, MA 02747, USA, bnotaros@umassd.edu

Abstract: Higher-order, large-domain electromagnetic simulations are presented based on the finite element method (FEM), method of moments (MoM), and physical optics (PO). The simulations combine higher order geometrical modeling and higher order field/current modeling, which is referred to as double-higher-order modeling. The examples demonstrate that accurate and efficient FEM, MoM, and PO simulations require both higher-order geometrical flexibility for curvature modeling and higher-order basis functions for field/current modeling in the same method. It is optimal to have the geometrical orders and current/field approximation orders of the elements entirely independent from each other, so that the two sets of parameters can be combined independently in a double-higher-order model.

Key words: electromagnetic analysis, finite-element methods, moment methods, physical optics, higher-order modeling.

1. Introduction

This paper discusses higher order modeling of geometry and higher order modeling of fields and currents in the framework of the finite element method (FEM), method of moments (MoM), and physical optics (PO). Traditional FEM, MoM, PO, and hybrid simulation tools are low-order or small-domain (subdomain) computational techniques. In the small-domain approach, structures are modeled by volume and surface geometrical elements (finite and boundary elements) that are electrically very small (typically, on the order of $\lambda/10$ in each dimension, λ being the wavelength in the medium) and the fields and currents over the elements are approximated by low-order (zeroth-order and first-order) basis functions. This results in a very large number of unknowns (unknown field- or current-distribution coefficients) needed to obtain results of satisfactory accuracy, with all the associated problems and enormous requirements in computational resources. In addition, commonly used finite and boundary elements are in the form of cells (bricks, tetrahedra, and triangular prisms) with planar sides and flat (triangular and quadrilateral) patches, and thus they do not provide enough flexibility and efficiency in modeling of structures with pronounced curvature. According to the higher-order or large-domain computational approach, on the other side, a structure is approximated by a number of as large as possible geometrical elements, and the approximation of field/current components within individual elements is in the form of a single (three- or two-fold) functional series of sufficiently high order (e.g., [1-5]). This approach can greatly reduce the number of unknowns for a given problem and enhance further the accuracy and efficiency of the analysis in practical applications.

We present our higher-order, large-domain FEM [4], MoM [5], and hybrid MoM-PO techniques, which are referred to as double-higher-order methods because they combine higher order geometrical modeling and higher order field/current modeling. They enable using large curved FEM hexahedral volume

Report Documentation Page

Form Approved
OMB No. 0704-0188

1. REPORT DATE	2. REPORT TYPE	3. DATES COVERED
23 APR 2004	**N/A**	**-**

4. TITLE AND SUBTITLE
Higher Order Geometrical Modeling and Higher Order Field/Current Modeling in FEM, MoM, and PO Simulations

5a. CONTRACT NUMBER
5b. GRANT NUMBER
5c. PROGRAM ELEMENT NUMBER

6. AUTHOR(S)

5d. PROJECT NUMBER
5e. TASK NUMBER
5f. WORK UNIT NUMBER

7. PERFORMING ORGANIZATION NAME(S) AND ADDRESS(ES)
University of Massachusetts Dartmouth, Electrical and Computer Engineering Dept. 285 Old Westport Road, North Dartmouth, MA 02747, USA,

8. PERFORMING ORGANIZATION REPORT NUMBER

9. SPONSORING/MONITORING AGENCY NAME(S) AND ADDRESS(ES)

10. SPONSOR/MONITOR'S ACRONYM(S)

11. SPONSOR/MONITOR'S REPORT NUMBER(S)

12. DISTRIBUTION/AVAILABILITY STATEMENT
Approved for public release, distribution unlimited

13. SUPPLEMENTARY NOTES
See also ADM001763, Annual Review of Progress in Applied Computational Electromagnetics (20th) Held in Syracuse, NY on 19-23 April 2004., The original document contains color images.

14. ABSTRACT

15. SUBJECT TERMS

16. SECURITY CLASSIFICATION OF:			17. LIMITATION OF ABSTRACT	18. NUMBER OF PAGES	19a. NAME OF RESPONSIBLE PERSON
a. REPORT	b. ABSTRACT	c. THIS PAGE			
unclassified	**unclassified**	**unclassified**	**UU**	**6**	

Standard Form 298 (Rev. 8-98)
Prescribed by ANSI Std Z39-18

elements and MoM and PO quadrilateral surface elements that are on the order of λ (e.g., 1.5λ – 2λ) in each dimension as building blocks for modeling of the electromagnetic structure (i.e., the finite/boundary elements can be by three/two orders of magnitude larger in volume/area than traditional low-order elements). Element orders in the model, however, can also be low, so that the lower-order modeling approach is actually included in the higher-order modeling. The examples demonstrate that for FEM, MoM, and PO modeling of general structures that may possess arbitrary curvature it is essential to have both higher-order geometrical flexibility for curvature modeling and higher-order basis functions for field/current modeling in the same method. In addition, it is optimal to have the geometrical orders and field/current approximation orders of the elements entirely independent from each other, so that the two sets of parameters of the double-higher-order model can be combined independently for the best overall performance of the method.

2. Higher Order Volume and Surface Geometrical Modeling

As basic building blocks for volume geometrical modeling in FEM, we use generalized curved parametric hexahedra [4] of higher (theoretically arbitrary) geometrical orders. A generalized hexahedron (Fig. 1) is analytically described as

$$\boldsymbol{r}(u,v,w)=\sum_{i=1}^{M}\boldsymbol{r}_i\hat{L}_i^{K_{uvw}}(u,v,w)=\sum_{m=0}^{K_u}\sum_{n=0}^{K_v}\sum_{l=0}^{K_w}\boldsymbol{r}_{mnl}\,u^m v^n w^l\,,\quad -1\le u,v,w\le 1,\quad M=(K_u+1)(K_v+1)(K_w+1)\,,\quad (1)$$

where $\boldsymbol{r}_1$, $\boldsymbol{r}_2$, …, $\boldsymbol{r}_{\mathrm{M}}$ are the position vectors of the interpolation nodes, and K_u, K_v, and K_w (K_u, K_v, $K_w \ge 1$) are geometrical orders of the element along u-, v-, and w- parametric coordinates, respectively. The functions $\hat{L}_i^{K}(u,v,w)$ are defined as

$$\hat{L}_i^{K_{uvw}}(u,v,w)=L_m^{K_u}(u)L_n^{K_v}(v)L_l^{K_w}(w)\,,\quad i=m+n(K_u+1)+l(K_u+1)(K_v+1)+1\,,\qquad (2)$$

where $L_m^{K_u}$, $L_n^{K_v}$, and $L_l^{K_w}$ represent Lagrange interpolating polynomials.

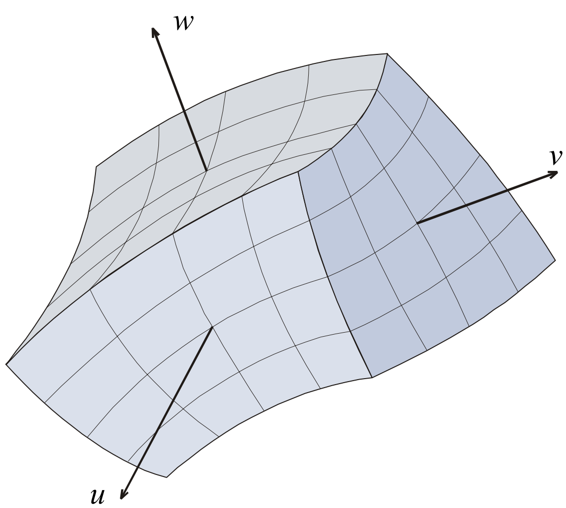

Fig. 1. A generalized curved parametric hexahedron of arbitrary geometrical orders for FEM volumetric modeling.

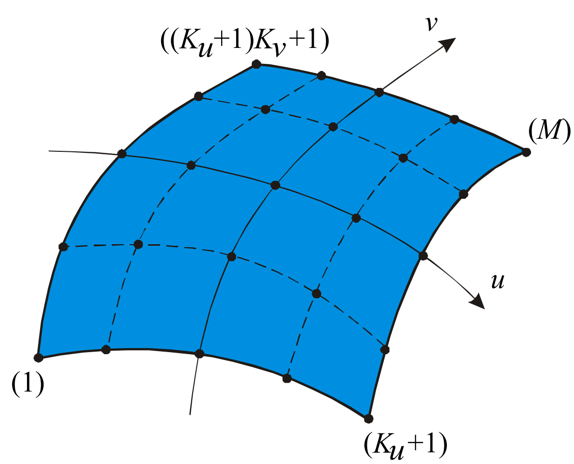

Fig. 2. A generalized curved parametric quadrilateral of arbitrary geometrical orders for modeling of MoM and PO surfaces.

Surface geometrical modeling in MoM and PO is carried out using generalized curved parametric quadrilaterals of higher (theoretically arbitrary) geometrical orders K_u and K_v [5]. A generalized quadrilateral (Fig. 2) is analytically described by the 2-D version of Eqs.(1) and (2).

3. Higher Order Field and Current Modeling

The electric fields inside the FEM hexahedra are represented as [4]

$$\boldsymbol{E} = \sum_{i=0}^{N_u-1}\sum_{j=0}^{N_v}\sum_{k=0}^{N_w} \alpha_{uijk}\, \boldsymbol{f}_{uijk} + \sum_{i=0}^{N_u}\sum_{j=0}^{N_v-1}\sum_{k=0}^{N_w} \alpha_{vijk}\, \boldsymbol{f}_{vijk} + \sum_{i=0}^{N_u}\sum_{j=0}^{N_v}\sum_{k=0}^{N_w-1} \alpha_{wijk}\, \boldsymbol{f}_{wijk} \quad , \tag{3}$$

where N_u, N_v, and N_w are the adopted degrees of the field approximation, which are entirely independent from the element geometrical orders, K_u, K_v, and K_w, and $\boldsymbol{f}$ are curl-conforming hierarchical vector basis functions defined as

$$\boldsymbol{f}_{uijk} = u^i P_j(v) P_k(w)\, \boldsymbol{a}'_u, \quad \boldsymbol{f}_{vijk} = P_i(u) v^j P_k(w)\, \boldsymbol{a}'_v, \quad \boldsymbol{f}_{wijk} = P_i(u) P_j(v) w^k\, \boldsymbol{a}'_w, \quad P_i(u) = \begin{cases} 1-u, & i=0 \\ u+1, & i=1 \\ u^i-1, & i\ge 2, \text{even} \\ u^i-u, & i \ge 3, \text{odd} \end{cases}$$

$$\boldsymbol{a}'_u = \frac{\boldsymbol{a}_v \times \boldsymbol{a}_w}{J}, \quad \boldsymbol{a}'_v = \frac{\boldsymbol{a}_w \times \boldsymbol{a}_u}{J}, \quad \boldsymbol{a}'_w = \frac{\boldsymbol{a}_u \times \boldsymbol{a}_v}{J}, \quad J = (\boldsymbol{a}_u \times \boldsymbol{a}_v)\cdot \boldsymbol{a}_w, \quad \boldsymbol{a}_u = \frac{\partial \boldsymbol{r}}{\partial u}, \quad \boldsymbol{a}_v = \frac{\partial \boldsymbol{r}}{\partial v}, \quad \boldsymbol{a}_w = \frac{\partial \boldsymbol{r}}{\partial w}. \tag{4}$$

In MoM, electric and magnetic surface current density vectors over every generalized quadrilateral in the model are represented as [5]

$$\boldsymbol{J}_{\mathrm{S}} = \sum_{i=0}^{N_u}\sum_{j=0}^{N_v-1} \alpha_{uij}\, \boldsymbol{f}_{uij} + \sum_{i=0}^{N_u-1}\sum_{j=0}^{N_v} \alpha_{vij}\, \boldsymbol{f}_{vij}, \quad \boldsymbol{M}_{\mathrm{S}} = \sum_{i=0}^{N_u}\sum_{j=0}^{N_v-1} \beta_{uij}\, \boldsymbol{f}_{uij} + \sum_{i=0}^{N_u-1}\sum_{j=0}^{N_v} \beta_{vij}\, \boldsymbol{f}_{vij} \ , \tag{5}$$

where N_u and N_v are the adopted degrees of the current approximation and $\boldsymbol{f}$ are divergence-conforming hierarchical vector basis functions defined as

$$\boldsymbol{f}_{uij} = \frac{P_i(u) v^j}{J} \boldsymbol{a}_u, \quad \boldsymbol{f}_{vij} = \frac{u^i P_j(v)}{J} \boldsymbol{a}_v, \quad J = |\boldsymbol{a}_u \times \boldsymbol{a}_v|. \tag{6}$$

In PO, basis functions for approximating $\boldsymbol{J}_{\mathrm{S}}$ are divergence-conforming two-dimensional interpolatory Chebyshev-type polynomials given by

$$\boldsymbol{f}_{uij} = \frac{C_{uij}}{J} \frac{\mathrm{T}^{\mathrm{mod}}_{Nu+1}(u)}{u-u_i^{\mathrm{mod}}} \frac{\mathrm{T}_{Nv}(v)}{v-v_j} \boldsymbol{a}_u, \quad \boldsymbol{f}_{vij} = \frac{C_{vij}}{J} \frac{\mathrm{T}_{Nu}(u)}{u-u_i} \frac{\mathrm{T}^{\mathrm{mod}}_{Nv+1}(v)}{v-v_j^{\mathrm{mod}}} \boldsymbol{a}_v, \tag{7}$$

where $\mathrm{T}^{\mathrm{mod}}$ and T are the modified and regular Chebyshev polynomials, respectively, and C_{ij} are the normalization factors. The zeros of modified polynomials, u_i^{mod}, are obtained by scaling the zeros of regular Chebyshev polynomials by a factor of $\cos\{\pi/[2(N_u+1)]\}$, and similarly for v_j^{mod}.

In FEM and MoM, the same functions $\boldsymbol{f}$ are used for testing, which gives rise to the Galerkin method. In PO, a modified point-matching technique is applied at the interpolation points of the basis functions, which makes the extremely large PO-PO projection matrix in the general MoM-PO matrix system be an identity matrix, and thus tremendously reduces the computational costs associated with electromagnetic interactions in the PO region. In addition, the implemented point-matching testing in the PO region has proved to be accurate enough in all applications and is faster than the Galerkin procedure.

4. Numerical Results and Discussion

As an example of higher order FEM modeling of curved structures, Fig. 3 shows the average percentage error in calculating k_0 for the first eleven modes of an air-filled metallic spherical cavity, versus the number of unknowns for the solution (the error is given with respect to the exact result). The numerical results are shown for a higher order FEM solution with the sphere modeled by a single generalized hexahedron of the 2nd geometrical order ($K_u = K_v = K_w = 2$) and two higher order single-element solutions using a generalized hexahedron of the 4th geometrical order ($K_u = K_v = K_w = 4$). In the first 4th-order geometrical model, the control (interpolating) points that do not belong to the cavity surface (hexahedron faces) are arranged to define an inscribed half-radius sphere, while in the second 4th-order geometrical model the inner control points define an inscribed cube with the spatial diagonal equal in length to the cavity radius. In all three models, the field-approximation orders are varied from $N_u = N_v = N_w = 3$ to $N_u = N_v = N_w = 7$ (p-refinement). Note that these are literally entire-domain FEM models (an entire computational domain is represented by a single finite element). We observe from the figure excellent convergence properties of all higher order solutions, namely, that the computation error decreases rapidly and monotonically when using p-refinement. We also observe a significant additional improvement in accuracy as a result of using geometrical modeling of the 4th order instead of the 2nd order geometrical modeling. In other words, it is impossible to p-refine the higher order model with the 2nd geometrical order below about 1% error in calculating k_0 due to the inherent geometrical error of the model, whereas the p-refinement in the model with the 4th geometrical order brings the analysis error quickly down to a fraction of a percent. Finally, we note that the 4th order geometrical model with the inner points on a cube, having less distorted coordinate lines throughout its volume and thus being able to represent the fields more accurately, yields by an order of magnitude smaller average error in the low-error region than the model with the inner points placed on a sphere, which is an indication of the importance of careful meshing considerations when elements of higher geometrical orders are used.

As an example of higher order MoM modeling of curved structures, consider a spherical dielectric scatterer 1 m in radius in the frequency range 10 – 600 MHz [5]. The relative permittivity of the dielectric is $\varepsilon_r = 2.25$ (polyethylene). Shown in Fig. 4 is the RCS of the sphere calculated using two higher order models with the sphere surface being approximated by means of 384 generalized quadrilaterals of the first geometrical order ($K_u = K_v = 1$) and 6 generalized quadrilaterals of the fourth geometrical order ($K_u = K_v = 4$), respectively, along with the analytical solution in the form of Mie's series. The adopted electric and magnetic current approximation orders in the first model are $N_u = N_v = 2$ in all elements, and the resulting total number of unknowns is 6144. In the second model, $N_u = N_v = 5$ in all elements, which corresponds to a total of 2400 unknowns. We observe a very good agreement of the numerical results obtained by the higher order model with first-order geometrical modeling and the analytical results, with the RCS numerical predictions being slightly shifted toward higher frequencies. We also note that, even though this is an almost small-domain application of our large-domain MoM, where a relatively large number (384) of elements (with relatively low current approximation orders) is needed for the sphere surface to be geometrically accurately represented by parametric surfaces of the first geometrical order, the largest quadrilateral elements in the model are $0.39\lambda_{\text{free-space}}$ or $0.58\lambda_{\text{diel}}$ on a side ($\lambda_{\text{diel}} = \lambda_{\text{free-space}}/\sqrt{\varepsilon_r}$) at the highest frequency considered, which is still considerably above the usual small-domain limit of 0.1λ. On the other hand, the agreement of the model with fourth-order geometrical modeling with the exact solution is excellent in the entire frequency range considered. Note that the curved quadrilateral elements in this model are about $1.57\lambda_{\text{free-space}}$ or $2.35\lambda_{\text{diel}}$ across at the highest frequency. Note also that with the use of the model with fourth-order geometry modeling and fifth-order current modeling the number of unknowns is reduced about 2.5 times and the accuracy is increased as compared to the model with first-order geometry modeling and second-order current modeling.

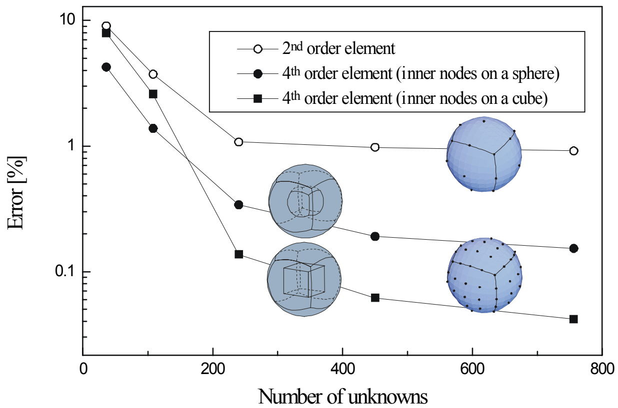

Fig. 3. Comparison of three higher order single-element (entire-domain) FEM solutions – average errors for the first eleven modes, k_0, of a spherical cavity against the number of unknowns.

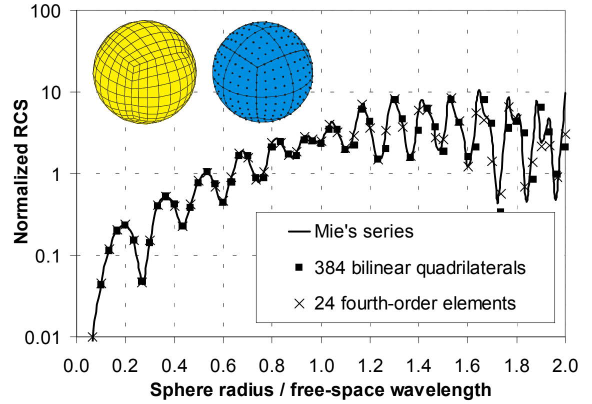

Fig. 4. Normalized radar cross-section [RCS/($a^2\pi$)] of a dielectric ($\varepsilon_r = 2.25$) sphere, for two higher-order, large-domain MoM models, along with the exact solution (Mie's series).

As an example of higher order PO modeling of curved structures, consider an antenna system consisting of an array of nine λ/2 dipoles in front of a circular metallic cylinder (Fig. 5). The radius of the cylinder is 7.5λ and its height 12λ. The dipoles are parallel to the cylinder axis and are situated 1.25λ from the cylinder surface with an angular separation of 3.75 degrees between the adjacent dipoles in the array. All of the dipoles are center-fed by point generators of equal amplitudes and phases. The lateral surface (barrel) of the cylinder is approximated using 144 quadrilaterals of the second geometrical orders ($K_u = K_v = 2$) and each of the cylinder bases (caps) is represented by a total of 24 second-order and 36 first-order ($K_u = K_v = 1$) geometrical elements, with the seventh-order current approximation in both parametric coordinates ($N_u = N_v = 7$) for all of the quadrilaterals in the model. All quadrilaterals are approximately 2λ on a side, which is 20 times the usual low-order limit of λ/10. Each dipole is modeled using two straight wire segments with fourth-order current approximations ($N_u = 4$). In the hybrid MoM-PO analysis, the dipole array is in the MoM region and the cylinder is in the PO region. Fig. 6 shows the computed radiation pattern of the array in the horizontal plane. The results obtained by the higher order MoM-PO technique are compared with the results of the pure MoM analysis. We observe an excellent agreement of the two sets of results in the front region (for angles up to 90 degrees). In the back region (for angles between 90 and 180 degrees), however, the MoM-PO prediction is not accurate enough. The discrepancy between the pure MoM and hybrid MoM-PO here is certainly primarily due to the fact that the currents over the parts of the cylinder surface in the shadow region, which are quite weak as compared to the currents in the lit region but contribute significantly to the (low-field) radiation in the back region of the antenna system, are set to be zero in the MoM-PO simulation. Using the two-fold symmetry of the problem, the total number of unknowns for the antenna system amounts to 6181 with both techniques. In the pure MoM analysis, the CPU time is about 19 minutes with a relatively modest PC (AMD XP-1700+ with 512 MB of RAM). In the hybrid MoM-PO analysis, the number of unknowns in the MoM region is 20 and that in the PO region 6461. The CPU time is about 2 seconds with the same PC, which is by three orders of magnitude faster than with the rigorous (full MoM) higher order technique. Note also that the estimated number of unknowns, based on a topological analysis, for a common low-order small-domain MoM-PO solution with RWG basis functions on flat triangular patches and the use of two-fold symmetry is more than 65000 for the analysis of the same problem.

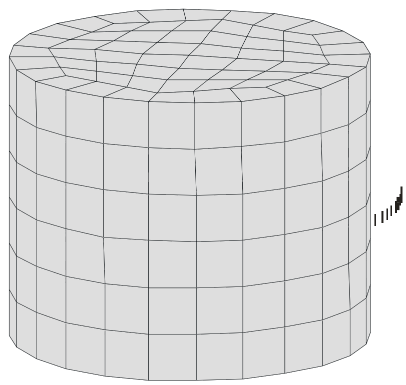

Fig. 5. Higher-order, large-domain MoM-PO geometrical model of an antenna system consisting of an array of nine λ/2 dipoles in front of a large metallic cylinder of finite length.

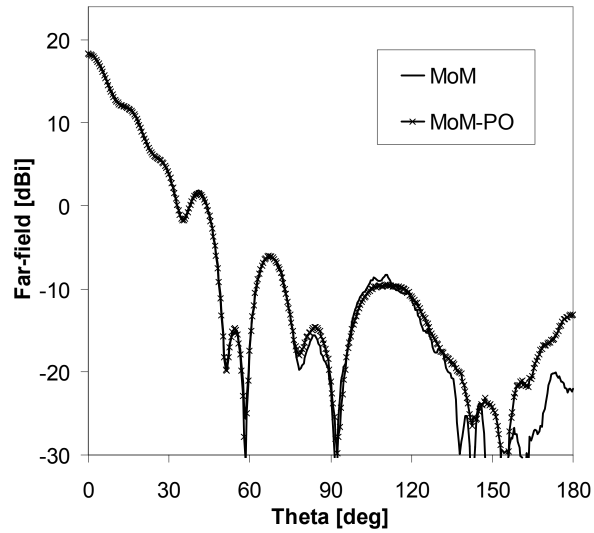

Fig. 6. Far field of the antenna system in Fig. 5, computed by the full MoM and hybrid MoM-PO higher-order techniques, respectively, in the horizontal plane.

5. Conclusions

This paper has presented higher-order, large-domain electromagnetic simulations based on the finite element method, method of moments, and physical optics. The implemented analysis tools are double-higher-order computational techniques that combine higher order geometrical modeling and higher order field/current modeling, which have been shown to be equally important for accurate and efficient FEM, MoM, and PO computations.

References

[1] B. M. Notaroš and B. D. Popović, “General entire-domain method for analysis of dielectric scatterers”, *IEE Proceedings - Microwaves, Antennas and Propagation*, Vol. 143, No. 6, pp.498-504, December 1996.

[2] B. M. Notaroš and B. D. Popović, “Large-domain integral-equation method for analysis of general 3D electromagnetic structures”, *IEE Proceedings - Microwaves, Antennas and Propagation*, Vol. 145, No. 6, pp.491-495, December 1998.

[3] B. M. Notaroš, B. D. Popović, J. Peeters Weem, R. A. Brown, and Z. Popović, “Efficient large-domain MoM solution to electrically large practical EM problems”, *IEEE Transactions on Microwave Theory and Techniques*, Vol. 49, No. 1, pp. 151-159, January 2001.

[4] M. M. Ilić and B. M. Notaroš, “Higher Order Hierarchical Curved Hexahedral Vector Finite Elements for Electromagnetic Modeling”, *IEEE Transactions on Microwave Theory and Techniques*, Vol. 51, No. 3, pp. 1026-1033, March 2003.

[5] M. Djordjević and B. M. Notaroš, “Double-Higher-Order Method of Moments for Surface Integral Equation Modeling of Metallic and Dielectric Antennas and Scatterers”, accepted for publication in the *IEEE Transactions on Antennas and Propagation*.

